

## LETTERS

# *Toxoplasma* co-opts host gene expression by injection of a polymorphic kinase homologue

J. P. J. Saeij<sup>1\*</sup>, S. Collier<sup>1\*</sup>, J. P. Boyle<sup>1</sup>, M. E. Jerome<sup>2</sup>, M. W. White<sup>2</sup> & J. C. Boothroyd<sup>1</sup>

*Toxoplasma gondii*, an obligate intracellular parasite of the phylum Apicomplexa, can cause severe disease in humans with an immature or suppressed immune system. The outcome of *Toxoplasma* infection is highly dependent on the strain type, as are many of its *in vitro* growth properties<sup>1</sup>. Here we use genetic crosses between type II and III lines to show that strain-specific differences in the modulation of host cell transcription are mediated by a putative protein kinase, ROP16. Upon invasion by the parasite, this polymorphic protein is released from the apical organelles known as rhoptries and injected into the host cell, where it ultimately affects the activation of signal transducer and activator of transcription (STAT) signalling pathways and consequent downstream effects on a key host cytokine, interleukin (IL)-12. Our findings provide a new mechanism for how an intracellular eukaryotic pathogen can interact with its host and reveal important differences in how different *Toxoplasma* lineages have evolved to exploit this interaction.

Most *Toxoplasma gondii* isolates that have been identified in Europe and North America belong to three distinct clonal lines<sup>2,3</sup>, referred to as types I, II and III. The three types differ widely in a number of phenotypes in mice such as virulence, persistence, migratory capacity, attraction of different cell types and induction of cytokine expression<sup>1</sup>. Recent results indicate that such differences might also exist in human infection<sup>4–9</sup>. To test the hypothesis that some of these strain-specific differences are a result of how the strains interact with the host cell, we infected human foreskin fibroblasts (HFFs) with each of the three types and used microarray analysis to investigate differences in host gene expression 24 h later. Significance analysis of microarrays<sup>10</sup> (SAM) identified 105 human complementary DNAs, representing at least 88 unique genes that were regulated in a strain-specific manner (false discovery rate 15%) (Fig. 1a).

If the strain-specific regulation of a host gene has a genetic basis, it should segregate among F1 progeny derived from a cross between two strains that differ in its regulation. We therefore infected HFFs separately with each of 19 F1 progeny derived from crosses between type II and type III parasites and repeated the microarray analyses. The F1 strains formed two distinct clusters and, for a large portion of the genes, the progeny belonging to each cluster modulated human gene expression in either a type II- or a type III-like manner (Fig. 1b).

To identify the loci involved in this differential regulation, we performed a genome-wide scan for association of *Toxoplasma* genetic markers<sup>11</sup> and the expression level of each of the 42,000 human cDNAs on the microarray using the package R/qtl (ref. 12). From this, 3,188 cDNAs could be mapped to a specific *Toxoplasma* genomic locus (Fig. 2a–c). Interestingly, 1,176 of those cDNAs mapped to chromosome VIIb (Fig. 2b) and, of these, 617 had their highest logarithm of odds (LOD) score around genetic markers L339 and L363 (see Fig. 2c for an example). This indicated that, in the vicinity

of these markers, there is at least one polymorphic *Toxoplasma* gene whose product has a strong effect on gene expression in HFFs. This was also corroborated by the fact that all F1 progeny in cluster 1 of Fig. 1b have type III alleles for markers L339 and L363 while all in cluster 2 have type II alleles.

Pathway analysis showed that the group of human genes whose strain-specific modulation mapped to *Toxoplasma* chromosome VIIb was significantly enriched for genes involved in the IL-6, Janus kinase (JAK)/STAT, amyloid processing and IL-4 signalling pathways (Fischer's exact test for all was  $P < 5 \times 10^{-3}$ ; see Supplementary Fig. 2a–e). A broader, network analysis of molecular relationships between genes and gene products resulted in high scores for three networks whose central transcription factors were STAT3 and STAT5b (network 1), JUN (network 2) and hypoxia-inducible factor (HIF)-1A (network 3) (see Supplementary Fig. 2f–h). Given these results and the fact that the IL-4 and IL-6 signalling pathways culminate in the activation of the transcription factors STAT6 and STAT3, respectively<sup>13</sup>, we hypothesized that a large part of the strain-specific regulation of host genes is due to differences in how

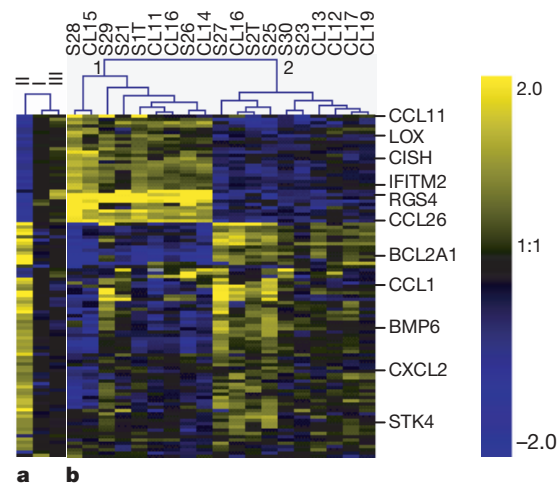


**Figure 1 | *Toxoplasma* strain-specific regulation of human gene expression.** **a**, HFFs were infected with type I, type II or type III *Toxoplasma* strains. 24 h after infection, expression profiles were obtained using human cDNA arrays. The averaged results (from at least three biological replicates) for median-centred expression levels for cDNAs are displayed using a  $\log_2$  blue (low) to yellow (high) scale. Values  $\log_2 > 2$  or  $\log_2 < -2$  were assigned the values 2 and -2, respectively. **b**, HFFs were infected with 19 F1 progeny derived from crosses (S or CL) between type II and type III strains. Details are as for **a**. Also displayed is the unsupervised clustering of experiments. For a full-size image and array data see Supplementary Fig. 1 and Supplementary data 1.

<sup>1</sup>Department of Microbiology and Immunology, Fairchild Building D305, 300 Pasteur Drive, Stanford University School of Medicine, Stanford, California 94305-5124, USA.

<sup>2</sup>Department of Veterinary Molecular Biology, College of Agriculture, Montana State University, Bozeman, Montana 59717, USA.

\*These authors contributed equally to this work.

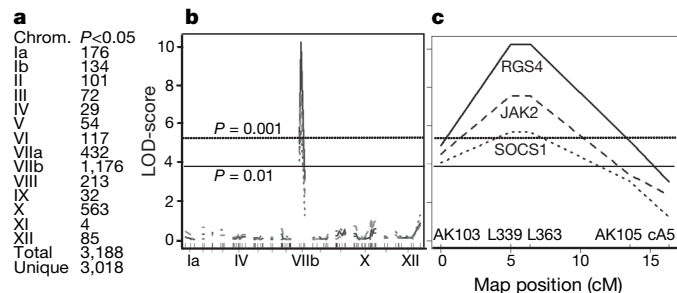


**Figure 2 | Genome-wide scans for association of human gene expression with *Toxoplasma* genetic markers.** **a**, For each *Toxoplasma* chromosome, the number of cDNAs that mapped significantly ( $P < 0.05$ , permutation test) to a genetic marker on that chromosome is shown. **b**, Plots indicate the log-likelihood association of expression of the human cDNAs for *RGS4* (solid line), *JAK2* (dashed line) and *SOCS1* (dotted line) with markers aligned across the entire *Toxoplasma* genome in chromosome order. Selected chromosomes are indicated. **c**, An enlargement of Fig. 2b focusing on chromosome VIIb with the names of genetic markers indicated. LOD-score profiles of all significantly mapped human genes are provided as Supplementary data 2.

the different *Toxoplasma* strains intersect the STAT activation pathways, although from the network analysis it is clear that other transcription factors are also probably involved (for example, JUN and HIF1A).

To test whether differences in STAT activation are central to the strain-specific differences, we analysed HFFs infected with type I, II or III parasites using immunofluorescence assays (IFA) and western blotting with antibodies specific for the tyrosine-phosphorylated (activated) forms of STAT3 and STAT6. Both methods revealed that,

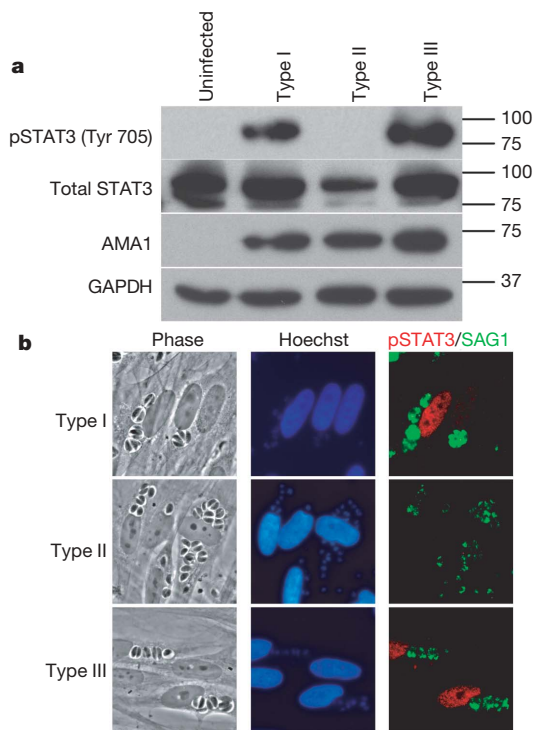


**Figure 3 | Strain-specific activation of STAT3.** **a**, Western blot analysis of strain-dependent phosphorylation of STAT3. Serum-starved HFFs were infected with a type I, type II or type III *Toxoplasma* strain and 18 h after infection cells were lysed and analysed by immunoblotting. GAPDH (host cell-specific) and AMA1 (parasite-specific) levels are shown as loading controls. **b**, Immunofluorescence analysis of strain-dependent activation of STAT3. HFFs were infected with type I, II or III parasites (MOI 10) for 18 h, fixed and incubated with antibodies against parasite SAG1 or the phosphorylated forms of STAT3 (Tyr 705).

18 h after infection, serum-starved HFFs infected with type I or type III strains contain much more activated STAT3 and STAT6 (not shown) than HFFs infected with type II strains (Fig. 3 a, b). At earlier time points (for example, 1 h after infection), HFFs individually infected with any of the three strains showed nuclear localization of tyrosine-phosphorylated STAT3 (data not shown). Somehow, late in infections and with type II parasites only, it seems that phospho-STAT3 Tyr 705 levels in the nucleus drop, presumably because tyrosine phosphorylation is repressed or reversed. In all cases, activation of STAT3 and STAT6 depended on parasite invasion, as uninfected neighbouring cells showed little or no signal. Co-infection of HFFs with type II and type III strains showed strong phosphorylation of STAT3 and STAT6, showing that this is an active property of type I and III strains and that type II strains cannot repress this process (not shown).

To confirm and refine the preliminary mapping of the *Toxoplasma* genomic region involved in activation of STAT3/6, parasites that had recombinations in the region of interest on chromosome VIIb were genotyped and phenotyped for their capacity to activate STAT3/6. These data allowed us to narrow down the locus involved to a region between L363 and AK104, representing a maximum size of 0.56 Mb (see Supplementary Fig. 3). This interval on VIIb contains 78 predicted proteins (<http://www.toxodb.org>). Assuming that the crucial gene encodes a polymorphic, secreted protein that can substantially alter host cell transcription, we identified *ROP16* as the most likely candidate. First, there are 57 single-nucleotide polymorphisms (SNPs; 34 of which are non-synonymous) between the type II allele of *ROP16* and the type I and III alleles, which are virtually identical (5 SNPs), consistent with the genetic evidence that the type II allele functions completely differently from those of types I and III (see Supplementary Fig. 4). Second, ROP16 has high homology to serine/threonine protein kinases, which are potent modulators of many cell functions. And, third, ROP16 localizes to the *Toxoplasma* rhoptries<sup>14</sup>, a set of apical organelles that can secrete vesicle-like bodies (termed ‘evacuoles’) into the host cell upon invasion<sup>15</sup>.

To characterize ROP16 further, a type I strain was engineered to express a carboxy-terminally haemagglutinin (HA)-tagged version of the protein derived from either a type I or type II background; the resulting strains were designated type I:ROP16<sub>I</sub> and type I:ROP16<sub>II</sub>, respectively. IFA showed that the tagged ROP16 was correctly targeted to the rhoptries and that within 10 min of invasion it had entered the host cell nucleus; it was still visible at 24 h but the brightest relative staining occurred between 10 min and 4 h (Fig. 4) with an apparent diminution of signal thereafter. Similar results were obtained when the mouse macrophage cell line RAW 264.7 was used as the host cell (not shown). Localization of HA-tagged ROP16 to the host cell nucleus depended on the putative nuclear localization signal

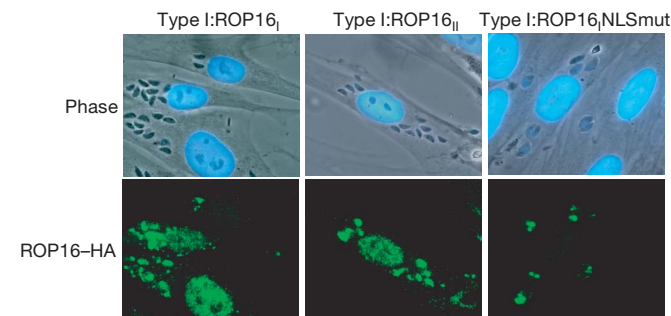


**Figure 4 | ROP16 is secreted from the parasite and localizes to the host cell nucleus.** Type I parasites expressing HA-tagged type I ROP16 (Type I:ROP16<sub>I</sub>, left), type II ROP16 (Type I:ROP16<sub>II</sub>, middle) or type I ROP16 with a mutated NLS (Type I:ROP16<sub>I</sub>NLSmut, right) were added (MOI 10) to HFFs and cells were fixed after 4 h. ROP16 was visualized using anti-HA antibodies followed by incubation with secondary (anti-rat Alexa 488) antibodies.

(NLS) in ROP16 (RKRKRK at residues 339–344, inclusive): mutation of lysine residues 340, 342 and 344 to methionines (yielding RMRMRM) markedly diminished nuclear localization (Fig. 4).

In both HFFs and macrophages, the intensity of ROP16 staining in the nucleus depended on the number of invasion events (as determined by the number of parasitophorous vacuoles), not the total number of parasites present, which increases as a function of time (Fig. 4 and data not shown). Combined with the fact that ROP16 reaches the nucleus within 10 min of initial contact, these data indicate that ROP16 is introduced during the invasion process and not in a slow, steady release from intracellular parasites. Recently, we have seen that a second rhopty protein, in this case a protein phosphatase,

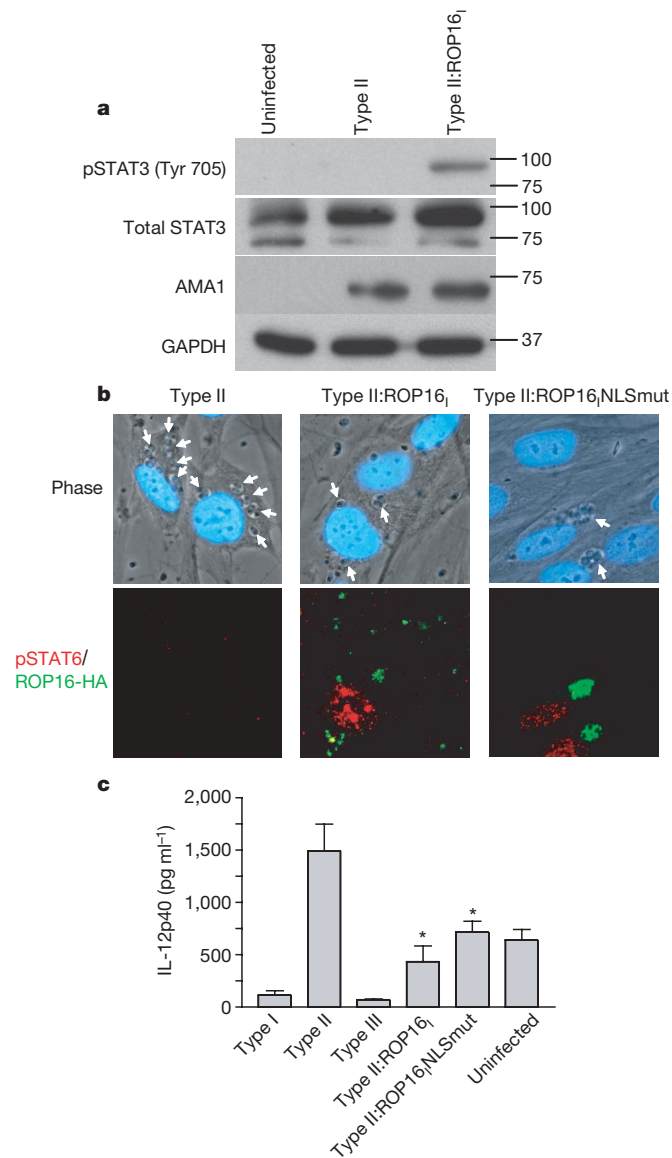


**Figure 5 | ROP16 mediates strain-specific activation of STAT3/6 and consequent downstream effects on IL-12. a**, Type II parasites expressing the type I ROP16 gene induce phosphorylation of STAT3. HFFs were infected with type II or type II:ROP16, and lysates were prepared for immunoblot analysis as described in the legend to Fig. 3a. **b**, Type II parasites expressing the normal type I ROP16 gene or the type I ROP16 NLS mutant gene induce translocation of phosphorylated STAT6 to the host cell nucleus. White arrows indicate parasites. **c**, Type II parasites expressing the type I ROP16 gene or the type I ROP16 NLS mutant gene inhibit the production of IL-12p40 from infected macrophages. Error bars represent s.e.m. of three replicates. Data shown are from one representative experiment out of three. Asterisks denote significantly less IL-12p40 production relative to type II parasites (Student's *t*-test).

is injected into host cells with similar kinetics to ROP16. It also possesses an NLS and reaches the host nucleus with similar kinetics<sup>16</sup>.

To test whether ROP16 is involved in the strain-specific activation of STAT3/6, we engineered type II strains to express an additional, type I allele of ROP16 (designated type II:ROP16<sub>i</sub>). Western blot and IFA revealed that, as before, HFFs infected with the parental type II strain showed little if any STAT3/6 activation 18 h after infection, whereas those infected with the type II:ROP16<sub>i</sub> showed strong activation in both assays (Fig. 5a, b). These experiments show that ROP16 has an important role in maintaining the activation of STAT3 and STAT6 in infected HFFs and indicate that the type I allele is probably dominant over the type II version.

Tyrosine phosphorylation of STAT3 and STAT6 generally occurs in the cytoplasm of a cell. It is therefore surprising that ROP16 seems to be concentrated in the host cell nucleus. To investigate whether nuclear localization is essential for its function, we engineered a type II strain to express a type I allele of ROP16 carrying the NLS disruption described above (RKRKRK to RMRMRM). Infection with the resulting strain, designated type II:ROP16<sub>i</sub>NLSmut, showed a comparable level of STAT6 activation as infection with the type II:ROP16<sub>i</sub> strain (Fig. 5b). These results indicate that ROP16 can probably execute its function in the cytosol (perhaps as it transits to the nucleus) although we cannot exclude the possibility that the small amount of ROP16 that still goes to the nucleus in the NLS mutant (not shown) is responsible for its function in cells infected with this strain.

To investigate how ROP16 mediates its effect on STAT3/6, we used a battery of antibodies that recognize the activated (phosphorylated) forms of proteins upstream of the STAT3/6 signalling pathways. We found no strain differences in the activation of extracellular signal regulated kinase (ERK)1/2, P38, Jun amino-terminal kinase (JNK), AKT, JAK2 and tyrosine kinase (TYK)2. Combined with the fact that all three strains activate STAT3/6 early (see above and Supplementary Fig. 5), these results indicate that the pathway that leads to the initial activation of these key transcription factors is similar between strains but that HFFs infected with type I/III strains are actively prevented from subsequent downregulation.

Our results provide a potential molecular basis for at least one of the strain-dependent differences in how a host cell responds to *Toxoplasma* infection: type II but not type I or III strains induce mouse macrophages to produce high levels of IL-12 (both p40 and p70; ref. 17) and constitutive activation of STAT3 by type I parasites prevents lipopolysaccharide-triggered production of IL-12p40 by macrophages<sup>18</sup>. To determine whether ROP16 is involved in these differences, we examined STAT3 phosphorylation and IL-12p40 production by murine RAW264.7 macrophages infected with our engineered parasites and stimulated with interferon (IFN)- $\gamma$  and LPS. The amount of phosphorylated STAT3 in macrophages infected with the different *Toxoplasma* strains paralleled the results described above for HFFs (see Supplementary Fig. 6). We confirmed that infection of macrophages with type II, but not with the type I or III strains, results in very high secretion of IL-12p40 and further showed that the type II:ROP16<sub>i</sub> and type II:ROP16<sub>i</sub>NLSmut strains elicit significantly less IL-12p40 than parental type II parasites (Fig. 5c), as predicted by our results showing increased activation of STAT3 by these strains. Such effects could be an important part of the different disease outcomes seen with the type I, II and III strains. The facts that the type II strain induced more IL-12p40 than IFN- $\gamma$  and LPS alone, and that the type II:ROP16<sub>i</sub> strain did not bring the IL-12p40 down to the levels of type I and III strains, indicate that in addition to ROP16, other molecules might be involved in the strain-specific regulation of IL-12p40.

To come full circle and show that because of or in addition to its role in strain-specific activation of STAT3/6, ROP16 is involved in the strain-specific differences originally observed in the human cDNA microarray experiments, we compared the gene expression profiles of HFFs infected with type II and type II:ROP16<sub>i</sub> strains.

Of 13,382 cDNAs that met the quality control threshold, 127 were previously shown (Fig. 2a) to map to chromosome VIIb with an average difference greater than twofold between the original F1 progeny based on which ROP16 allele they carried. Of these 127 cDNAs, 29 (out of 242 total) were differentially regulated (average of at least twofold difference in the two arrays) when comparing the type II and type II:ROP16, strains. This is significantly more genes than expected by chance (hypergeometric distribution,  $P < 10^{-15}$ ), confirming a role for ROP16 in this strain-specific regulation of host gene expression. Furthermore, all 29 genes changed in the expected direction (See Supplementary data 3).

The phenomenology of ROP16 introduction is analogous to type III and type IV secretion systems in prokaryotes<sup>19</sup> but there are no indications for the existence of such systems outside bacteria. One of the earliest events in *Toxoplasma* invasion is a break in the host cell membrane<sup>20</sup> and this might represent the moment when injection of ROP16 occurs, although we have been unable to detect ROP16 free in the cytosol or even associated with vacuoles<sup>15</sup> (data not shown). Our results do not reveal the primary target of ROP16. It probably does not directly phosphorylate STAT3/6 but instead is likely to intersect pathways that lead to or maintain such activation. This could involve something akin to what has been reported<sup>21</sup> for v-Abl, an oncogenic tyrosine kinase that causes constitutive activation of Jaks and STATs by disrupting suppressor of cytokine signalling (SOCS)-1 function (SOCS-1 normally targets Jaks and STATs for proteasomal degradation). Infection with type I and III strains results in a higher level of SOCS-1, SOCS-2 and SOCS-3 mRNA than infection with type II (see Supplementary data 2) and this difference maps to ROP16 (Fig. 2). This result is consistent with the fact that STAT3 is a positive regulator of SOCS (that is, the sustained activation of STAT3 results in their upregulation) and indicates that the mechanism involved in the type I and III-specific maintenance of activated STAT3 involves a block in SOCS function or some other downstream effect rather than a decrease in SOCS expression.

Rhoptries are a defining property of all Apicomplexa and some of the proteins found in the *Toxoplasma* rhoptries have homologues in *Plasmodium*. Thus, the ability to co-opt host cell gene expression for the parasite's own purposes might be found in other Apicomplexa that also are otherwise trapped within a membrane-limited vacuole (for example, *Plasmodium* species as they grow within hepatocytes). This represents a previously undescribed mechanism for interaction between eukaryotic pathogens and their hosts.

## METHODS

Details of parasite strains, genetic crosses and microarray analysis can be found in Supplementary Information.

**Immunofluorescence analysis.** Parasites were allowed to invade confluent HFF monolayers on coverslips for 0.17, 0.5, 1, 4, 6, 8, 18 or 24 h. The cells were then fixed, blocked and permeabilized. Coverslips were incubated with 3F10 (anti-HA) antibody, antibodies specific for the tyrosine phosphorylated forms of STAT3 and STAT6, or a mouse monoclonal antibody against surface antigen (SAG)-1 (DG52)<sup>22</sup>. Fluorescent secondary antibodies and Hoechst dye were used for antigen and DNA visualization, respectively.

**Western blots.** Parasites (MOI 10) were added to HFFs and infection was allowed to proceed for 18 h. Western blots were performed as described<sup>23</sup> using antibodies specific for total STAT3 (Cell Signaling Technologies), GAPDH (Calbiochem), AMA1 (mAb B3.90<sup>24</sup>) or for the phosphorylated forms of STAT3 (phospho-Tyr705) and STAT6 (phospho-Tyr641) (both from Cell Signaling Technologies).

**IL-12 enzyme-linked immunosorbent assay (ELISAs).** RAW264.7 macrophages were activated with IFN- $\gamma$  (20 U ml<sup>-1</sup>) and LPS (100 ng ml<sup>-1</sup>) and 1 h later parasites were added at a multiplicity of infection (MOI) of 10. After 24 h of infection, supernatants were collected and IL-12p40 ELISAs were performed as per manufacturer's recommendations (BD Biosciences).

Received 13 July; accepted 1 November 2006.

Published online 20 December 2006.

1. Saeji, J. P., Boyle, J. P. & Boothroyd, J. C. Differences among the three major strains of *Toxoplasma gondii* and their specific interactions with the infected host. *Trends Parasitol.* **21**, 476–481 (2005).

2. Howe, D. K. & Sibley, L. D. *Toxoplasma gondii* comprises three clonal lineages: correlation of parasite genotype with human disease. *J. Infect. Dis.* **172**, 1561–1566 (1995).
3. Darde, M. L., Bouteille, B. & Pestre-Alexandre, M. Isoenzyme analysis of 35 *Toxoplasma gondii* isolates and the biological and epidemiological implications. *J. Parasitol.* **78**, 786–794 (1992).
4. Grigg, M. E., Ganatra, J., Boothroyd, J. C. & Margolis, T. P. Unusual abundance of atypical strains associated with human ocular toxoplasmosis. *J. Infect. Dis.* **184**, 633–639 (2001).
5. Howe, D. K., Honore, S., Derouin, F. & Sibley, L. D. Determination of genotypes of *Toxoplasma gondii* strains isolated from patients with toxoplasmosis. *J. Clin. Microbiol.* **35**, 1411–1414 (1997).
6. Fuentes, I., Rubio, J. M., Ramirez, C. & Alvar, J. Genotypic characterization of *Toxoplasma gondii* strains associated with human toxoplasmosis in Spain: direct analysis from clinical samples. *J. Clin. Microbiol.* **39**, 1566–1570 (2001).
7. Khan, A. *et al.* Genotyping of *Toxoplasma gondii* strains from immunocompromised patients reveals high prevalence of type I strains. *J. Clin. Microbiol.* **43**, 5881–5887 (2005).
8. Darde, M. L., Villena, I., Pinon, J. M. & Beguinot, I. Severe toxoplasmosis caused by a *Toxoplasma gondii* strain with a new isoenzyme type acquired in French Guyana. *J. Clin. Microbiol.* **36**, 324 (1998).
9. Carme, B. *et al.* Severe acquired toxoplasmosis in immunocompetent adult patients in French Guiana. *J. Clin. Microbiol.* **40**, 4037–4044 (2002).
10. Tusher, V. G., Tibshirani, R. & Chu, G. Significance analysis of microarrays applied to the ionizing radiation response. *Proc. Natl Acad. Sci. USA* **98**, 5116–5121 (2001).
11. Khan, A. *et al.* Composite genome map and recombination parameters derived from three archetypal lineages of *Toxoplasma gondii*. *Nucleic Acids Res.* **33**, 2980–2992 (2005).
12. Broman, K. W., Wu, H., Sen, S. & Churchill, G. A. R/qtl: QTL mapping in experimental crosses. *Bioinformatics* **19**, 889–890 (2003).
13. Ihle, J. N. The Stat family in cytokine signaling. *Curr. Opin. Cell Biol.* **13**, 211–217 (2001).
14. Bradley, P. J. *et al.* Proteomic analysis of rhoptry organelles reveals many novel constituents for host-parasite interactions in *Toxoplasma gondii*. *J. Biol. Chem.* **280**, 34245–34258 (2005).
15. Hakansson, S., Charron, A. J. & Sibley, L. D. *Toxoplasma* vacuoles: a two-step process of secretion and fusion forms the parasitophorous vacuole. *EMBO J.* **20**, 3132–3144 (2001).
16. Gilbert, L. A., Ravindran, S., Turetzky, J. M., Boothroyd, J. C. & Bradley, P. J. *Toxoplasma gondii* targets a protein phosphatase 2C to the nucleus of infected host cells. *Eukaryot. Cell* (published online 3 November 2006; doi:10.1128/EC/00309-06).
17. Robben, P. M. *et al.* Production of IL-12 by macrophages infected with *Toxoplasma gondii* depends on the parasite genotype. *J. Immunol.* **172**, 3686–3694 (2004).
18. Butcher, B. A. *et al.* IL-10-independent STAT3 activation by *Toxoplasma gondii* mediates suppression of IL-12 and TNF- $\alpha$  in host macrophages. *J. Immunol.* **174**, 3148–3152 (2005).
19. Remaut, H. & Waksman, G. Structural biology of bacterial pathogenesis. *Curr. Opin. Struct. Biol.* **14**, 161–170 (2004).
20. Suss-Toby, E., Zimmerberg, J. & Ward, G. E. *Toxoplasma* invasion: The parasitophorous vacuole is formed from host cell plasma membrane and pinches off via a fission pore. *Proc. Natl Acad. Sci. USA* **93**, 8413–8418 (1996).
21. Limmander, A. *et al.* v-Abl signaling disrupts SOCS-1 function in transformed pre-B cells. *Mol. Cell* **15**, 329–341 (2004).
22. Burg, J. L., Perelman, D., Kasper, L. H., Ware, P. L. & Boothroyd, J. C. Molecular analysis of the gene encoding the major surface antigen of *Toxoplasma gondii*. *J. Immunol.* **141**, 3584–3591 (1988).
23. Chan, S. M. *et al.* Protein microarrays for multiplex analysis of signal transduction pathways. *Nature Med.* **10**, 1390–1396 (2004).
24. Mital, J. *et al.* Conditional expression of *Toxoplasma gondii* apical membrane antigen-1 (TgAMA1) demonstrates that TgAMA1 plays a critical role in host cell invasion. *Mol. Biol. Cell* **16**, 4341–4349 (2005).

**Supplementary Information** is linked to the online version of the paper at [www.nature.com/nature](http://www.nature.com/nature).

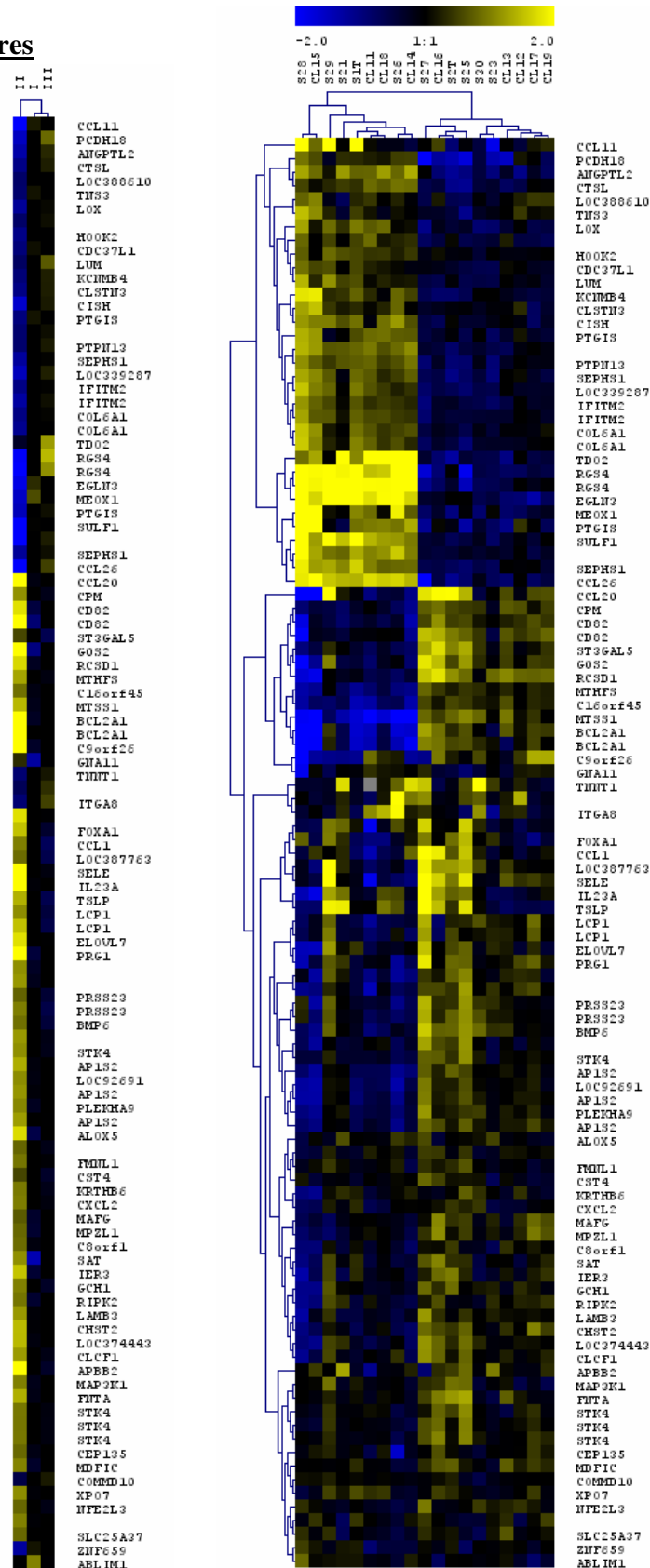
**Acknowledgements** This work was supported by grants from the NIH (to J.C.B., J.P.B. and M.W.W.), the Ellison Medical Foundation (to J.C.B.), the USDS (to M.W.W.) and the California Universitywide AIDS Research Program (to J.P.J.S. and S.C.). We thank K. Broman for help with R/qtl and the Stanford Functional Genomics Facility for the human cDNA microarrays used for this study.

**Author Contributions** J.P.J.S. and S.C. contributed equally to this work. J.P.J.S. performed the microarrays and pathway analyses. S.C. and J.P.J.S. performed the experiments in Fig. 3. S.C. performed the experiments in Fig. 4 and Fig. 5. J.P.B., M.E.J. and M.W.W. performed the genetic crosses that produced the progeny D3X1 and JD4. J.P.B. genotyped D3X1 and JD4. J.P.J.S., S.C., J.P.B. and J.C.B. wrote the paper. All authors discussed the results and commented on the manuscript.

**Author Information** The microarray data have been deposited in ArrayExpress with the accession number E-MEXP-783. Reprints and permissions information is available at [www.nature.com/reprints](http://www.nature.com/reprints). The authors declare no competing financial interests. Correspondence and requests for materials should be addressed to J.B. ([john.boothroyd@stanford.edu](mailto:john.boothroyd@stanford.edu)).

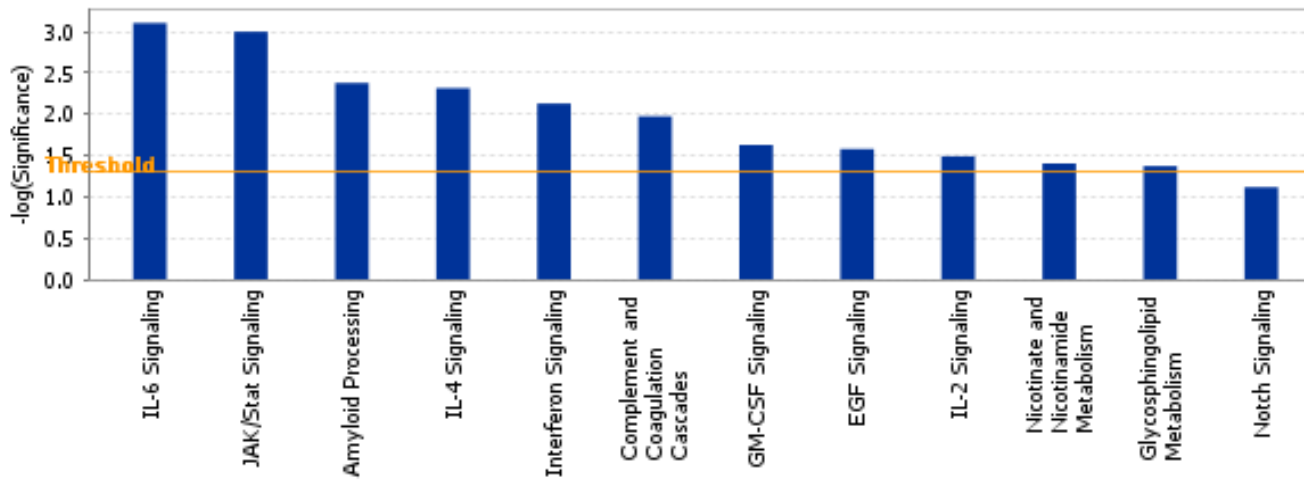
## SUPPLEMENTARY INFORMATION

## Supplementary Figures

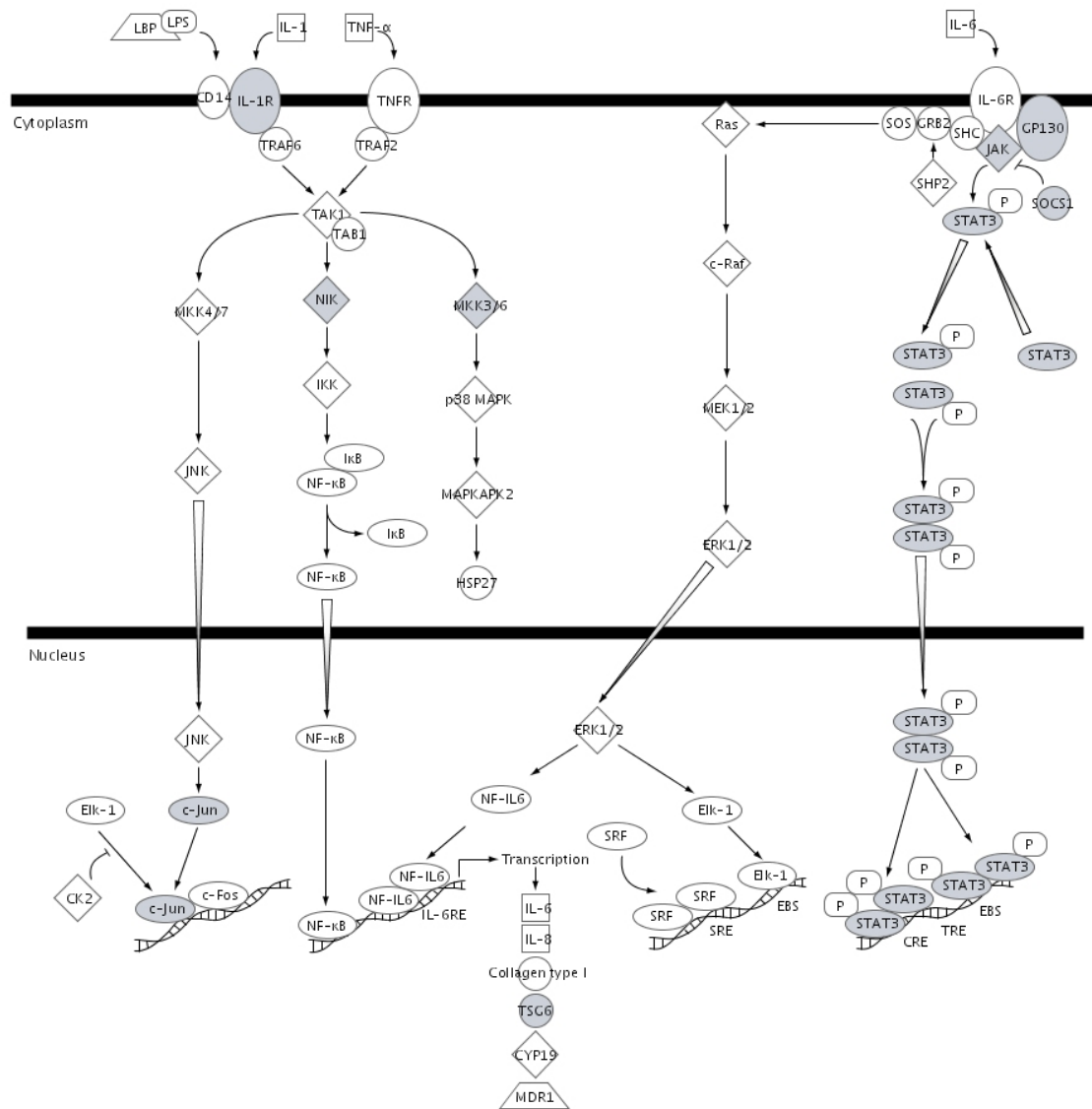


**Supplementary Figure 1.** This is an enlargement of Fig. 1. For details see Figure legend 1 and supplementary table 1.

Supplementary Figure 2a



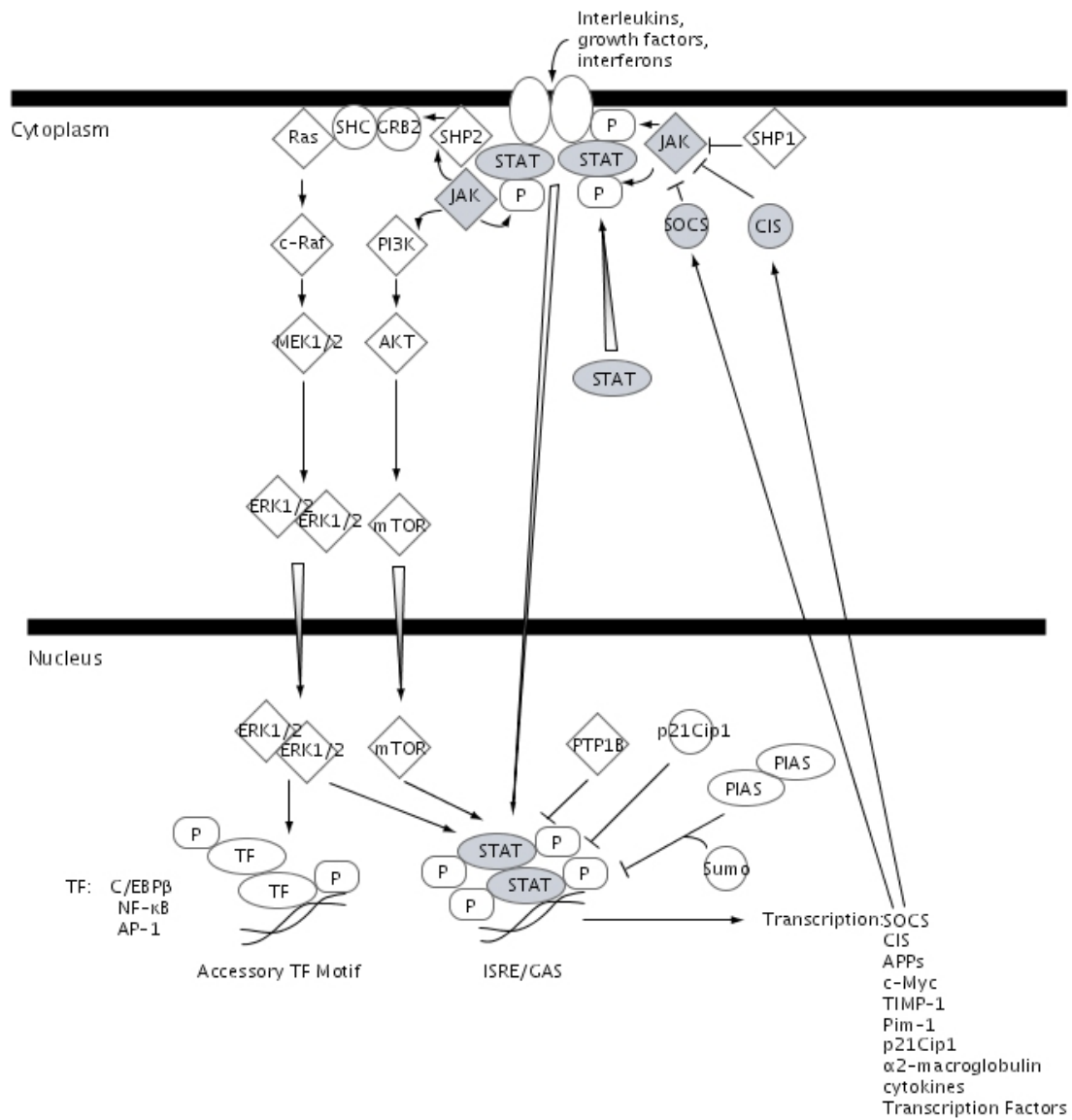
## IL-6 Signaling



Copyright Ingenuity Systems 2000 - 2005 All rights reserved.

Supplementary Figure 2b

## JAK/Stat Signaling

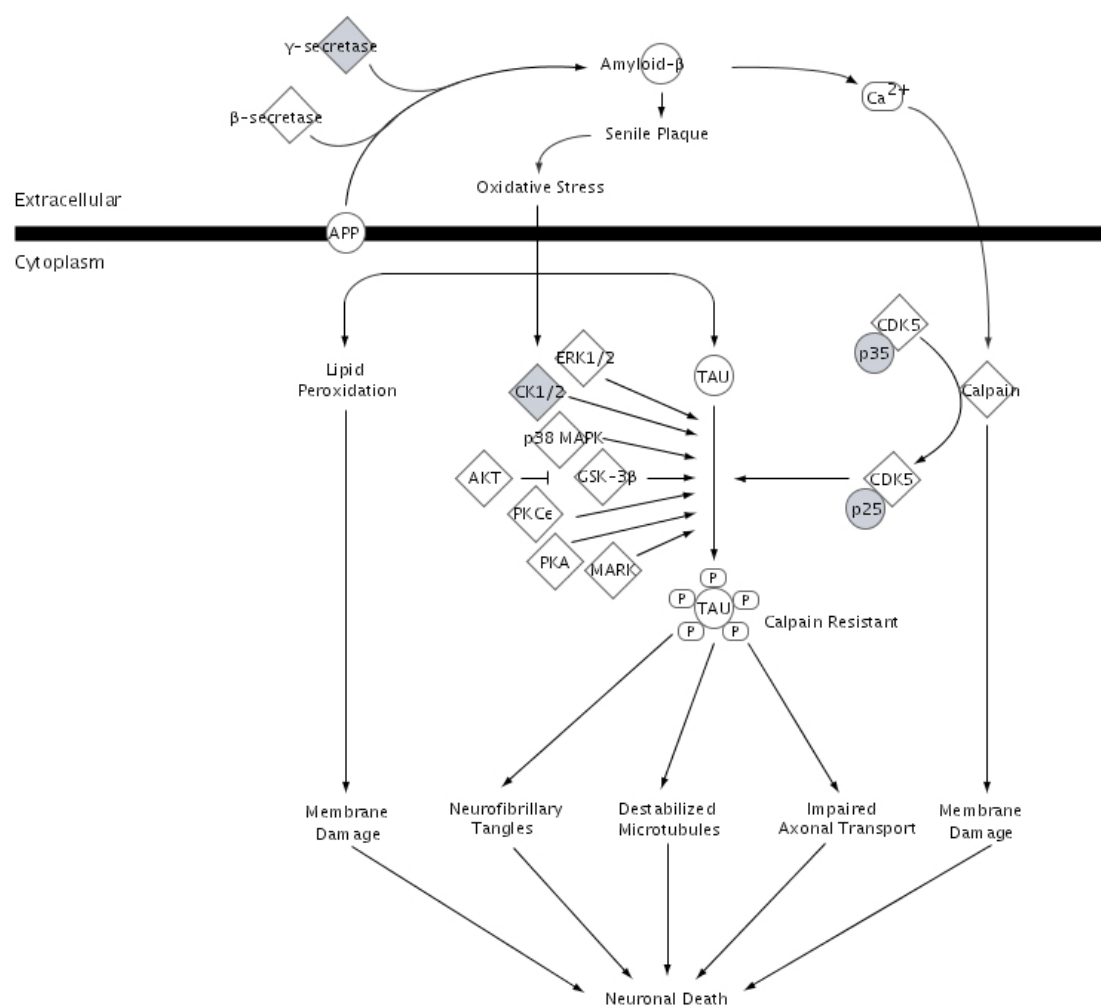


Copyright Ingenuity Systems 2000 - 2005 All rights reserved.

## Supplementary Figure 2c



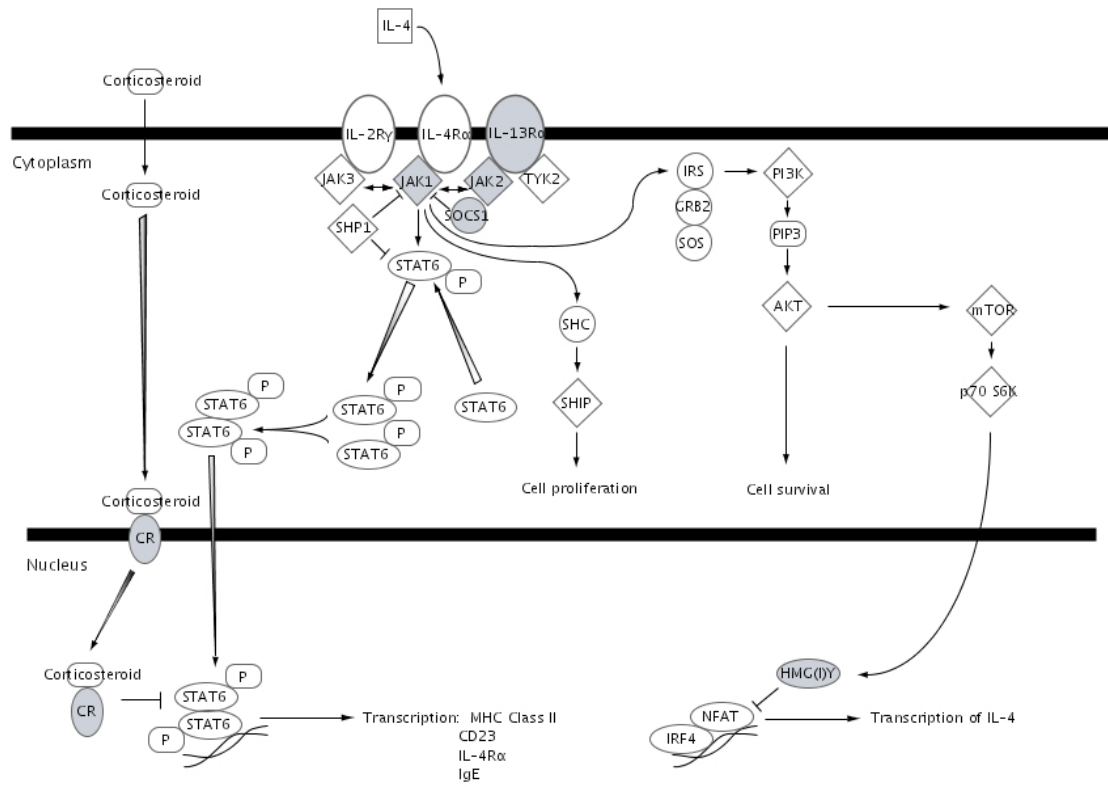
## Amyloid Processing



Copyright Ingenuity Systems 2000 - 2005. All rights reserved.

## Supplementary Figure 2d

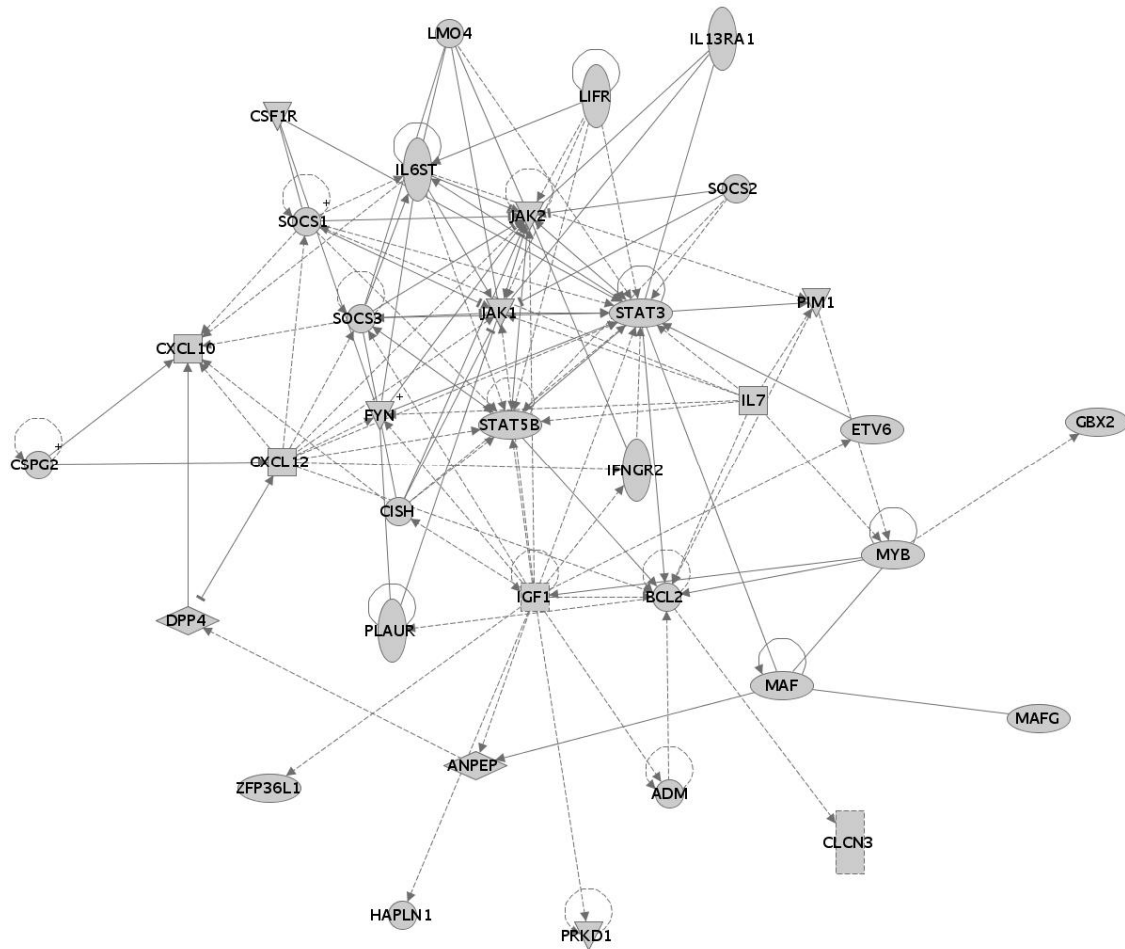
## IL-4 Signaling



Copyright Ingenuity Systems 2000 - 2005 All rights reserved.

Supplementary Figure 2e

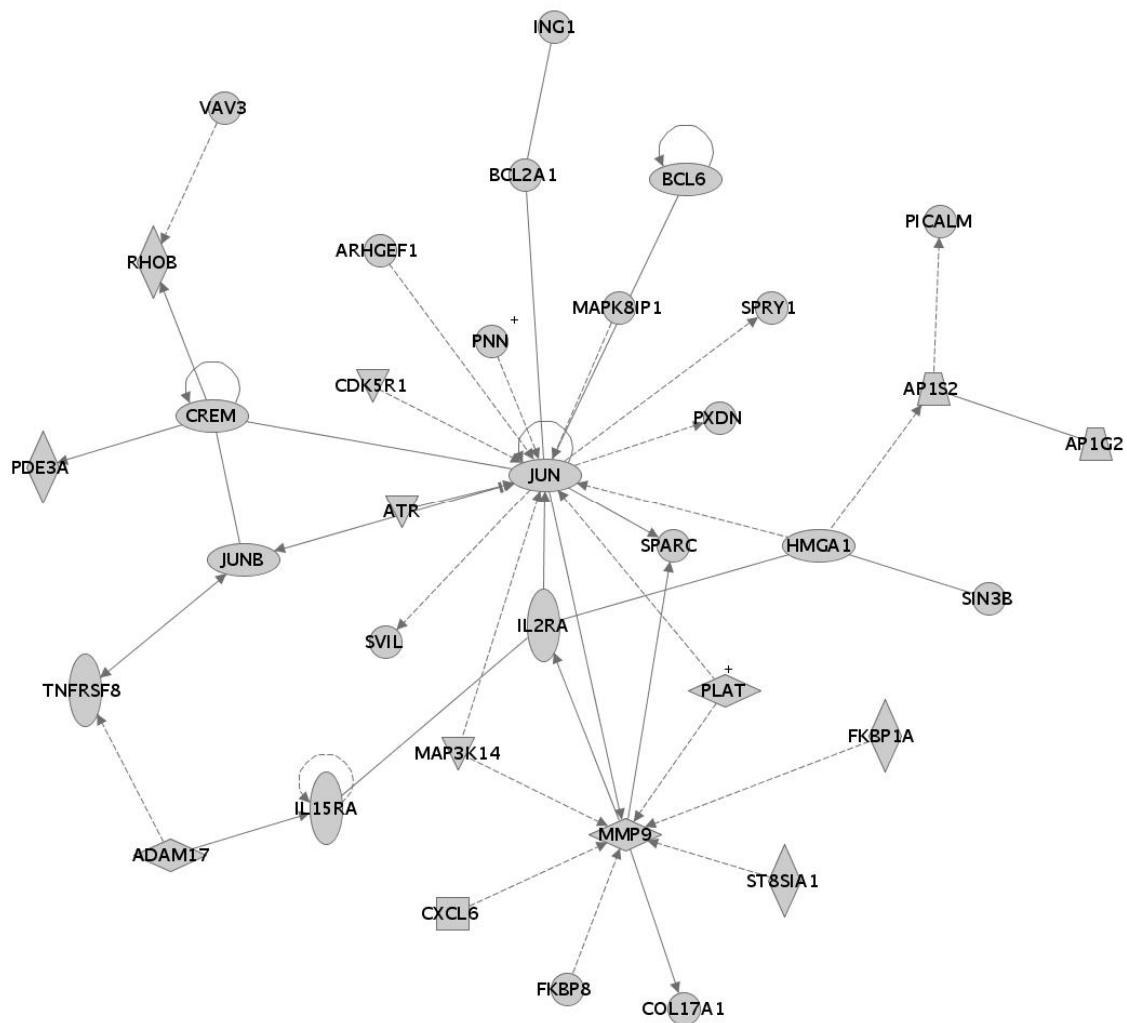
Viib100permp95 - 2006-03-23 03:23 PM: Viib100permp95.xls  
Network 1



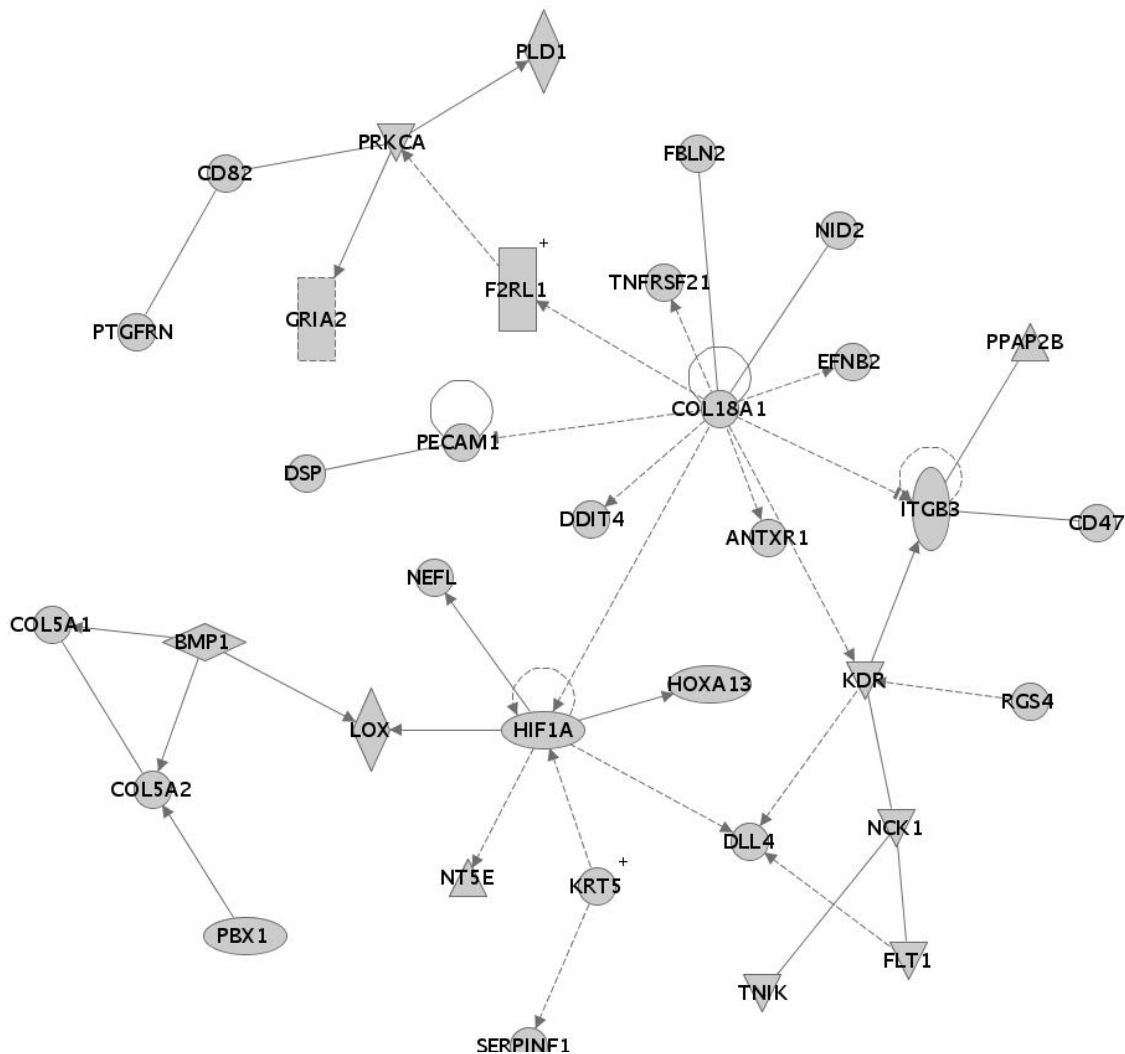
©2000-2005, Ingenuity Systems

Supplementary Figure 2f

Vii100permp95 - 2006-03-23 03:23 PM: Vii100permp95.xls  
Network 2



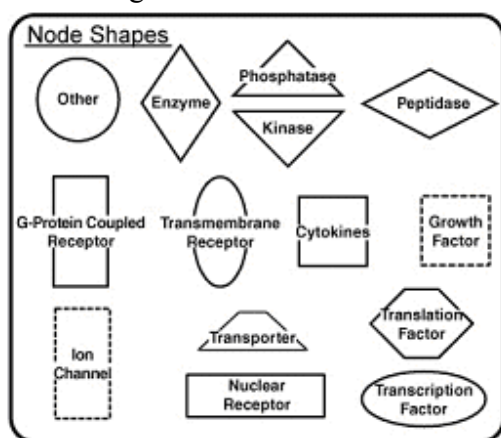
©2000–2005, Ingenuity Systems  
Supplementary Figure 2g



Supplementary Figure 2h

**Supplementary Figure 2. a**, Canonical pathways analysis identified the pathways from the Ingenuity Pathways Analysis library that were most significant to the dataset ([www.ingenuity.com](http://www.ingenuity.com)). Genes from the dataset that mapped to *Toxoplasma* chromosome VIIb (genome-wide P-value < 0.05) and were associated with a canonical pathway in the Ingenuity Pathways Knowledge Base were considered for the analysis. Fischer's exact test was used to calculate a P-value determining the probability that the association between the genes in the dataset and the canonical pathway is explained by chance alone. **b-e**, The human genes that mapped to *Toxoplasma* chromosome VIIb and contributed to the four pathways that appeared most significant in Suppl. Fig. 2a are drawn in grey. **f-h**, A data set containing the gene identifiers for the genes that mapped significantly to chromosome VIIb was uploaded and each gene identifier was mapped to its corresponding gene object in the Ingenuity Pathways Knowledge Base. These genes, called Focus Genes, were overlaid onto a global molecular network developed from information contained in the Ingenuity Pathways Knowledge Base. Networks of these

Focus Genes were then algorithmically generated based on their connectivity. A network/My Pathways is a graphical representation of the molecular relationships between genes/gene products. Genes or gene products are represented as nodes, and the biological relationship between two nodes is represented as an edge (line). All edges are supported by at least 1 reference from the literature, from a textbook, or from canonical information stored in the Ingenuity Pathways Knowledge Base. Human, mouse and rat orthologues of a gene are stored as separate objects in the Ingenuity Pathways Knowledge Base, but are represented as a single node in the network. Nodes are displayed using various shapes that represent the functional class of the gene product. Edges are displayed with various labels that describe the nature of the relationship between the nodes (e.g., P for phosphorylation, T for transcription). The three networks with the highest score are indicated.



| Marker   | Position | Strain |      |     |     |      |     |      |
|----------|----------|--------|------|-----|-----|------|-----|------|
|          |          | S23    | CL16 | S28 | S30 | D3XI | JD4 | KD11 |
| AK103    | 4996718  | 2      | 3    | 3   | 2   | 2    | 3   | 3    |
| 361*     | 4779775  | 2      | 2    | 3   | 2   | 2    | 3   | 3    |
| 615*     | 4724768  | 2      | 2    | 3   | 2   | 2    | 3   | 3    |
| 76*      | 4621257  | 2      | 2    | 3   | 2   | 2    | 3   | 3    |
| 920*     | 4527248  | 2      | 2    | 3   | 2   | 2    | 3   | 3    |
| L339     | 4466884  | 2      | 2    | 3   | 2   | 2    | 3   | 3    |
| L363     | 4158817  | 2      | 2    | 3   | 2   | 2    | 3   | 3    |
| 398*     | 3956443  | 2      | 2    | 3   | 2   | 2    | 2   | 3    |
| Rop16*   | 3954398  | 2      | 2    | 3   | 2   | 2    | 2   | 3    |
| 1060*    | 3792522  | 2      | 2    | 3   | 2   | 2    | 2   | 3    |
| 261*     | 3718397  | 2      | 2    | 3   | 2   | 2    | 2   | 3    |
| AK104    | 3603126  | 2      | 2    | 3   | 2   | 3    | 2   | 3    |
| 244*     | 3602023  | 2      | 2    | 3   | 2   | 3    | 2   | 3    |
| contig1* | 3456578  | 2      | 2    | 3   | 2   | 3    | 2   | 3    |
| 285*     | 3198244  | 2      | 2    | 3   | 2   | 3    | 2   | 3    |
| 377*     | 2893485  | 2      | 2    | 2   | 2   | 3    | 2   | 3    |
| AK105    | 2892714  | 2      | 2    | 2   | 2   | 3    | 2   | 3    |
| cA5-2    | 2497749  | 2      | 2    | 2   | 3   | 3    | 2   | 3    |

STAT6 Phenotype: - - + - - - +

**Supplementary Figure 3. Fine mapping of the *Toxoplasma* locus involved in strain-specific regulation of STAT6.** Genotyping of recombinant progeny at 18 markers. Markers with asterisks were made in our laboratory (sequences available upon request), and the rest of the markers have been used previously and are available at <http://toxomap.wustl.edu/>. All markers are present on the largest scaffold on chromosome VIIb (TGG\_995366; <http://www.toxodb.org>) and are presented in known order. Progeny were from crosses between a type II and a type III strain (S23, CL16, S28, S30, D3XI) or a backcross between S23 and a type III strain (JD4, KD11). STAT6 was detected in the nucleus of cells infected with the different strains as described in Materials and Methods. The limits of the region implicated by this analysis are denoted by a box.

```

#I MKVTTKGLAFALALLECTRCATARYMSFEEAQKASEAAKRQIATLPSDPSPLSNPGSRHRNRGGSPTAGQPSQSTLQPEQAAAEVGLGAG
#III .....
#II .....T.....K.....A.....

#I GSTQGQGRGTGGSAGAREERRSPSPE SAY PAT SSASLRGYQTQLSPSHLPPHSSGPGGWFPTESTYTLWSSPPQRLTHRKPSLSGVVVFTEF
#III .....Q.....
#II .....Q.....R.....F.P.....P.Q.....

#I QEPQEQYGAASSLASSPKGYVGGASSALS GKAVPT PASLGQENPLFPQSATLDSGIQS PAQKRRGSPQRQSAMPTGNPADSGASQLAF
#III .....
#II .....R.S.....V.....E.....I.S.E.....S

#I SHSSYVSVQASLAKRSEIRIRRVRLSEEGLEEVQQLKAAAQLLVAVPDYEMRAVLQEAVLSEQRVAARKRKRKQPPGAVESAVDEVFPP
#III .....
#II .V...A..TEHV.....T.....

#I NERVMMINANGVPIALYNRGLGSGHF GAVIKASLDDGTL YAAKV PYSQIVPNADATSAELEAGISSARAELVKTI RQELDVRDKLVAKG
#III .....
#II .....E.....

#I LTLTETVSQYGLPLCQMTLTL PENKATVVRGRSRLFVVSKEVMLLEPLIDGSAINSLVQSQPPFLFQRAVAREAILALAKLHELGF AHGDV
#III .....L.....
#II .....AE.....V.....PS.....I.....

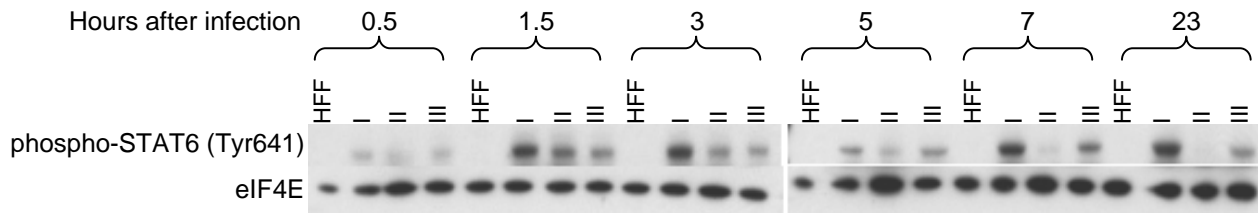
#I KLNMMIDVHGF GHMLDMG SVRPVDS CVSEEDKYYLR LWAPELAKSQHTSQKTC LKRGALDVWALGLAIFEFVCFNR L PYSLSNLPS SFW
#III .....
#II .....Q.....L.....

#I SRVEHLSRLRLSDFSVKDCNESDPAVMGIVVQFLNPDQP ERPELPKFVNSYTFQAPGVTSHLTRIPTTELS SHRM
#III .....A.....
#II .....A.....A.....N.E.....S.....R.....

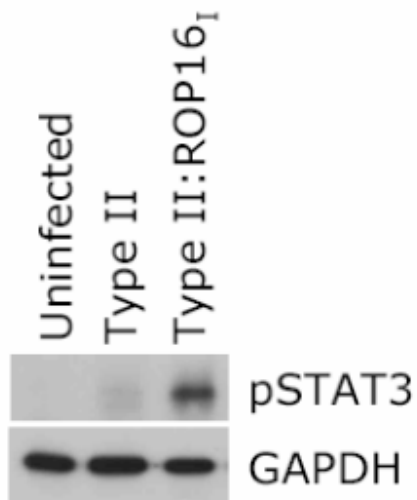
```

**Supplementary Figure 4.** The predicted amino acid sequence for the primary translation product of the *ROP16* gene is shown for type I parasites (top line). The sequences for types III and II are shown on the second and third lines, respectively with a dash to indicate identity to the type I sequence. The putative signal peptide is shown in blue (the cleavage site is predicted by SignalP<sup>28</sup>). A putative nuclear localization signal is in red (as predicted by PredictNLS<sup>29</sup>). Regions shown in magenta and light blue are the predicted ATP-binding and catalytic sites, respectively.





**Supplementary Figure 5.** Serum-starved HFFs were infected with a type I, type II or type III *Toxoplasma* strain (MOI 10) and at the indicated time-points after infection cells were lysed and analyzed by Western blotting with an antibody against phospho-STAT6 (Tyr641) (from Cell Signaling). An antibody against eIF4E was used as a loading control.



**Supplementary Figure 6.** RAW 264.7 macrophages were infected as described in the Materials and Methods for the HFF infections. These results demonstrate that in a similar manner as observed for HFFs, Type II parasites alone do not induce STAT3 phosphorylation in macrophages, but upon addition of the Type I ROP16 allele, infection induces activation of STAT3.

## **Supplementary Methods**

### **Parasites.**

Strains were maintained in vitro by serial passage on monolayers of HFFs as previously described<sup>30</sup>. The RH (type I), ME49 and Pru (both type II), CEP (type III) strains and the F1 recombinant progeny used in the microarray analyses, derived from crosses between ME49 and CEP<sup>31,32</sup>, have all been described previously.

**Genetic crosses.** Genetic crosses were carried out in cats as described previously<sup>31</sup>.

Briefly, *T. gondii* cysts were harvested from the brains of infected mice 24-30 days p.i. and fed in equal amounts to 6-10 week-old kittens. Feces were collected daily during days 3-8, and oocysts were floated on sucrose, washed, and allowed to sporulate for 3-8 days in 0.2% sulfuric acid. Sporozoites were excysted using standard protocols. For the backcross between the S23 strain (an F1 progeny clone of one of the previous type II x type III crosses<sup>31</sup>) and the type III strain (CL14), S23 was engineered to be resistant to FUdR by knocking out the gene for uracil phosphoribosyltransferase, and recombinants were selected by growth in FUdR (5 x 10<sup>-5</sup> M) and AraA (1.3 x 10<sup>-4</sup> M).

**Transgenic parasites.** Types I (RH) and II (Pru) parasites carrying a null mutant of the *HXGPRT* gene were transfected with the type I *ROP16* gene (from 2000 nt upstream of the predicted ATG start codon to the base pair immediately preceding the stop codon which was replaced with a single HA tag) cloned into the pHEX2 vector which provided the *SAG1* 3' UTR from the type I parasites and the *HXGPRT* gene. Transgenic parasites expressing *HXGPRT* were selected using normal cDMEM plus mycophenolic acid and xanthine as previously described<sup>33</sup>. A version of ROP16 carrying a mutated NLS was constructed by PCR amplification of type I ROP16 using primers with nucleotides encoding methionine (ATG) to replace the lysine (AAG) in the NLS sequence RKRKRK to RMRMRM (CGT ATG CGG ATG AGA ATG). The resulting ROP16 gene was cloned into the pHEX2 vector as described above.

**IFA.** Parasites were allowed to invade confluent HFF monolayers on coverslips for 0.17, 0.5, 1, 4, 6, 8, 18 or 24 h. The cells were then fixed (for nuclear localization, 4.0 % methanol-free formaldehyde for 20 min; for phospho-STAT analysis, 4.0 % methanol-free formaldehyde for 20 min followed by 100 % ice-cold methanol for 5 min), blocked in PBS supplemented with 3% BSA and permeabilized with 0.2% triton-X100 overnight at 4°C. Coverslips were then incubated with 3F10 (anti-HA) antibody (Roche, Palo Alto, CA), antibodies specific for the phosphorylated forms of STAT3 (phospho-Tyr705) and STAT6 (phospho-Tyr641) (Cell Signaling Technologies, Danvers, MA), or a mouse monoclonal antibody to SAG1 (DG52<sup>34</sup>), for 1-3 h at room temp. Fluorescent secondary antibodies (Invitrogen/ Molecular Probes, Carlsbad, CA) and Hoechst dye (Polysciences, Inc., Warrington, PA) were used for antigen and DNA visualization, respectively.

### **Microarrays: MIAME Checklist**

#### **Experiment Design**

The goal of the experiment: Genome-wide identification of *Toxoplasma* genomic loci mediating strain-specific modulation of host gene expression identifies ROP16 as a polymorphic *Toxoplasma* kinase that targets the host nucleus and co-opts transcription.

Brief description of the experiment: *Toxoplasma gondii*, an obligate, intracellular parasite of the phylum Apicomplexa, can cause severe disease in persons with an immature or

suppressed immune system. The majority of *Toxoplasma gondii* isolates so far identified within Europe and North America belong to three distinct clonal lines that differ in their fundamental virulence and disease presentation in mice and humans. We have determined that these three strains also differ substantially in how gene expression in the host cell is altered by infection. Using genetic crosses between a type II and type III strain, we have mapped the *Toxoplasma* loci involved and for one we have identified a polymorphic, secreted protein kinase (ROP16) as the responsible molecule involved. We show that upon invasion, this parasite kinase (ROP16) is injected into the host cytosol from the apical, secretory organelles known as rhoptries and that it then rapidly traffics to the host cell nucleus. Using transgenic parasites, we show that ROP16 affects activation of the STAT3 and STAT6 signalling pathways. Our findings provide a completely new mechanism for how an intracellular eukaryotic pathogen can interact with its host and co-opt gene expression. They also reveal major differences in how different *Toxoplasma* lineages have evolved to exploit this interaction.

Keywords: *Toxoplasma gondii*, strain comparison, human foreskin fibroblast, microarray, STAT, parasite

Experimental factors: *Toxoplasma gondii* genetic variation

Experimental design: Human Foreskin Fibroblasts (passage 10- 12) were infected with different *Toxoplasma gondii* strains and 24 h post-infection RNA was isolated. Indicated is which *Toxoplasma gondii* strains was used on each array and the multiplicity of infection (MOI) used (Strain\_Array\_MOI)

RH\_SHEM171\_MOI10 (Type I strain)  
RH\_SHEM173\_MOI5 (Type I strain)  
RH\_SHEM38\_MOI10 (Type I strain)  
RH\_SHEM86\_MOI10 (Type I strain)  
PDS\_SHEM137\_MOI10 (Type II strain)  
PDS\_SHEM139\_MOI10 (Type II strain)  
PDS\_SHEM82\_MOI10 (Type II strain)  
CTG\_SHEM140\_MOI10 (Type III strain)  
CTG\_SHEM175\_MOI10 (Type III strain)  
CTG\_SHEM83\_MOI10 (Type III strain)  
CTG\_SHEM84\_MOI10 (Type III strain)  
CL12\_SHFB243\_MOI10 (F1 recombinant progeny from Type II X Type III cross)  
CL13\_SHFB123\_MOI10 (F1 recombinant progeny from Type II X Type III cross)  
CL16\_SHFB170\_MOI10 (F1 recombinant progeny from Type II X Type III cross)  
CL17\_SHFB172\_MOI10 (F1 recombinant progeny from Type II X Type III cross)  
CL19\_SHFB173\_MOI10\_regrid (F1 recombinant progeny from Type II X Type III cross)  
S23\_SHFB245\_MOI10 (F1 recombinant progeny from Type II X Type III cross)  
S25\_SHFB215\_MOI10 (F1 recombinant progeny from Type II X Type III cross)  
S27\_SHFB213\_MOI10 (F1 recombinant progeny from Type II X Type III cross)  
S2T\_SHFB171\_MOI10 (F1 recombinant progeny from Type II X Type III cross)  
S30\_SHFB242\_MOI10 (F1 recombinant progeny from Type II X Type III cross)

CL14\_SHFB244\_MOI10 (F1 progeny from Type II X Type III cross, is identical to type III parent)  
CL15\_SHFB124\_MOI10 (F1 recombinant progeny from Type II X Type III cross)  
CL11\_SHFB174\_MOI10 (F1 recombinant progeny from Type II X Type III cross)  
S1T\_SHFB120\_MOI10 (F1 recombinant progeny from Type II X Type III cross)  
CL18\_SHFB211\_MOI10 (F1 recombinant progeny from Type II X Type III cross)  
S21\_SHFB214\_MOI10 (F1 recombinant progeny from Type II X Type III cross)  
S26\_SHFB212\_MOI10 (F1 recombinant progeny from Type II X Type III cross)  
S28\_SHFB121\_MOI10 (F1 recombinant progeny from Type II X Type III cross)  
S29\_SHFB122\_MOI10 (F1 recombinant progeny from Type II X Type III cross)

cDNA obtained from HFFs infected with the strains above was co-hybridized with cDNA made from Universal Human Reference RNA.

Gene expression of HFFs infected with a type II strain or a type II:ROP16<sub>1</sub> was compared by co-hybridization of cDNA derived from HFFs infected with each strain:

SHFB30 and SHFB32 are the corresponding arrays. The type II strains used were:

Prugniaud $\Delta$ HXGPRT and transgenic Prugniaud $\Delta$ HXGPRT complemented with a plasmid transfected with the type I ROP16 gene (2000 nt upstream of the predicted ATG start codon up to but not including the stop codon which was replaced with a single HA tag (TAC CCG TAC GAC GTC CCG GAC TAC GCG TAA) cloned into the pHEX2 vector which provided the SAG1 3' UTR from the type I parasites and the HXGPRT gene.

Quality control steps taken: For the Type I, II and III strain at least three independent biological replicates were performed.

#### **Samples used, extract preparation and labelling:**

Origin of each biological sample: Detailed information about the *Toxoplasma* strains used in this experiment can be found at: <http://www.toxomap.wustl.edu/>

The genotypes of the parasites used in this paper can be found at:

[http://www.toxomap.wustl.edu/IIxIII\\_Typing\\_Table.html](http://www.toxomap.wustl.edu/IIxIII_Typing_Table.html)

#### Manipulation of biological samples and protocols used:

Strains were maintained *in vitro* by serial passage on monolayers of human foreskin fibroblasts (HFFs) at 37°C in the presence of 5% CO<sub>2</sub>. HFFs were grown in Dulbecco modified Eagle medium (GIBCO BRL) supplemented with 10% NuSerum (Collaborative Biomedical Products), 2 mM glutamine, 50 µg/ml penicillin, 50 µg/ml streptomycin, and 20 µg/ml gentamicin (cDMEM).

Intracellular *Toxoplasma* from one T175 were isolated by scraping the monolayer.

Infected cells were spun down at 250 g for 10 min, supernatant was removed and cells resuspended in 4 ml of cDMEM. *Toxoplasma* were isolated from infected cells by syringe lysing them first through a 25 gauge needle and then through a 27 gauge needle. The isolated parasites were washed twice with 50 ml of PBS and resuspended in 5 ml of complete medium. After counting parasites, parasites (MOI 10) were added to confluent monolayers of HFFs in two separate T175 and infection proceeded for 24h.

The T175s that had most similar infection rates among the different F1 progeny were used for RNA extraction.

Experimental factor value for each experimental factor, for each sample: All samples were prepared 24 h after infection of HFFs with the different *Toxoplasma* strains.

Technical protocols for preparing the hybridization extract:

Total RNA was isolated from approximately  $10^7$  *Toxoplasma* infected human foreskin fibroblasts (HFFs) (one confluent T175) using Trizol (Invitrogen) according to the manufacturer's instructions, quantified by absorption spectroscopy and the integrity assessed by agarose gel electrophoresis. From this total RNA polyadenylated RNA was purified using Oligotex (QIAGEN, Valencia, CA). Microarray probes were prepared in two steps. First, cDNA was synthesized as follows: the total amount of polyadenylated RNA from one confluent T175 was mixed with 4  $\mu\text{g}$  of oligo-dT18VN primer in a total volume of 25  $\mu\text{l}$ , heated to 70°C for 10 min and cooled on ice. To this sample, we added dNTP, DTT, 5x reaction-mix and 1  $\mu\text{l}$  of superscript II reverse transcriptase. After a 1-h incubation at 42 °C another 1  $\mu\text{l}$  of superscript II RT was added and the reaction was incubated for another hour at 42 °C. RNA was degraded using Rnase H and RNase cocktail. The concentration of cDNA was estimated by running 2.5  $\mu\text{l}$  on an agarose gel next to a known amount of DNA ladder. Subsequently, 300 ng cDNA was labeled with Cy5-dUTP using random nonamers and DNA pol I Klenow. Universal human reference RNA was processed in the same manner and 250 ng cDNA was labeled with Cy3-dUTP. We added Cot1 Human DNA (Gibco-BRL), yeast tRNA and poly-A RNA (all, 20  $\mu\text{g}$ ), combined both probes, and purified the probe by centrifugation in a Centricon-30 micro-concentrator (Amicon) tubes.

### Hybridization procedures and parameters

Arrays were rehydrated by placing them face down in a humid chamber with 100 ml 1X SSC covered chamber with lid. They were rehydrated until array spots glisten, approximately 5-15 minutes. Subsequently, they were snap-dried (DNA side up) on a 70-80°C inverted heat block for 3 seconds and the DNA was UV crosslinked to glass with Stratalinker set for 65 mJ. Prehybridization was done in 5x SSC, 0.1 mg/ml BSA, 0.1% SDS at 42°C for 60 min. (300 ml MQ H<sub>2</sub>O, 100 ml filtered 20 x SSC, 4 ml 10mg/ml BSA stock solution (filtered), 4 ml 10% SDS, prewarmed in 42°C waterbath for 60 min). After 60 min. arrays were washed in H<sub>2</sub>O (three times), placed for 5 min in isopropanol and dried by centrifugation.

Hybridization solution (5.95  $\mu\text{l}$  20 X SSC, 1.05  $\mu\text{l}$  SDS) was added to the probe and H<sub>2</sub>O added to a total volume of 35  $\mu\text{l}$ . Then this solution was put at 100 °C for 2 min, centrifugated and added on top of a microarray. Sequence-verified human cDNA arrays (SHFB and SHEM series, 42,000 spots) were produced at Stanford. Hybridizations were performed under 22x60 mm cover slips at 65 °C in a humidified chamber for 16-20 h (with 4 drops of 3X SSC added to each corner to prevent dry-out). The coverslip was removed in 2x SSC, 0.03% SDS (40 °C) and Hybridized arrays were washed vigorously as follows: one wash for 5 min with 2X SSC (40 °C), once for 5 min with 1X SSC (37°C), and 1 times for 5 min with 0.1X SSC at room temperature. Arrays were dried by centrifugation for 2 min in a slide-rack in a Sorval RT7 plus centrifuge at 700 rpm.

### Measurement data and specifications

Data: Raw data will become available at the Stanford Microarray Database (SMD) (<http://genome-www5.stanford.edu/>)

Normalized and summarized data: The normalized and summarized data is attached in supplementary data 1,2,3

Data extraction and processing protocols: Arrays were scanned using a GenePix 4000A microarray scanner, controlled by GenePix Pro 5.1 software with a pixel size of 10  $\mu\text{m}$  and two-pass sequential line averaging. Laser power was set to 100% and PMT gains were adjusted during prescan to maximize effective dynamic range and to limit image saturation. To extract data from microarray scans, previously stored image files were gridded using Genepix 5.1 and uploaded into Stanford Microarray Database<sup>35</sup> (SMD).

Normalization, transformation and data selection procedures and parameters:

Although changing the normalization method or the parameters for data extraction can change the exact list of genes mentioned in this paper to some extent, this did not lead to substantial alterations in the results of the analyses.

The significance analysis of microarrays (SAM) algorithm with a false discovery rate (FDR) < 15% was used to identify significantly regulated genes. We did the following SAM analyses, one three class comparing I, II and III and all three possible two class comparisons (Type I vs II/III; Type II vs I/III, Type III vs II/I). cDNAs that had a FDR < 15% were pooled and the microarray data were analyzed using the 'Multi Experiment Viewer' – MeV version 3.1, included in the TM4 software package from The Institute of Genomic Research (<http://www.tigr.org/>).

To identify *Toxoplasma* genomic loci involved in strain-specific modulation of host expression a genome-wide scan for association of *Toxoplasma* genetic markers and the expression level of each of the 42,000 cDNAs on the microarray was performed using the program R and the package R/qtI. Genome-wide significance levels for each cDNA were determined by 100 permutations.

### **Array design**

General array design: SHEM and SHFB human cDNA arrays produced at Stanford were used for all the experiments. The arrays are printed with print tip type Majer 17-4 ss on Ultra GAPS slides coated with Corning amino-silane.

### Supplementary Notes

J.P.J.S was supported by a grant from the University of California Universitywide AIDS Research Program (F04-ST-216).

28. Bendtsen, J. D., Nielsen, H., von Heijne, G. & Brunak, S. Improved prediction of signal peptides: SignalP 3.0. *J Mol Biol* **340**(4), 783-95 (2004).
29. Cokol, M., Nair, R. & Rost, B. Finding nuclear localization signals. *EMBO Rep* **1**(5), 411-5 (2000).
30. Roos, D. S., Donald, R. G., Morrissette, N. S. & Moulton, A. L. Molecular tools for genetic dissection of the protozoan parasite *Toxoplasma gondii*. *Methods Cell Biol* **45**, 27-63 (1994).
31. Sibley, L. D., LeBlanc, A. J., Pfefferkorn, E. R. & Boothroyd, J. C. Generation of a restriction fragment length polymorphism linkage map for *Toxoplasma gondii*. *Genetics* **132**, 1003-15 (1992).
32. Khan, A. et al. Composite genome map and recombination parameters derived from three archetypal lineages of *Toxoplasma gondii*. *Nucleic Acids Res* **33**, 2980-92 (2005).
33. Donald, R. G., Carter, D., Ullman, B. & Roos, D. S. Insertional tagging, cloning, and expression of the *Toxoplasma gondii* hypoxanthine-xanthine-guanine phosphoribosyltransferase gene. Use as a selectable marker for stable transformation. *J Biol Chem* **271**, 14010-9. (1996).
34. Burg, J. L., Perelman, D., Kasper, L. H., Ware, P. L. & Boothroyd, J. C. Molecular analysis of the gene encoding the major surface antigen of *Toxoplasma gondii*. *J Immunol* **141**, 3584-91 (1988).
35. Ball, C. A. et al. The Stanford Microarray Database accommodates additional microarray platforms and data formats. *Nucleic Acids Res* **33**(Database issue), D580-2 (2005).